

Ground states of model core-softened colloids

This article has been downloaded from IOPscience. Please scroll down to see the full text article.

2008 J. Phys.: Condens. Matter 20 494220

(<http://iopscience.iop.org/0953-8984/20/49/494220>)

View [the table of contents for this issue](#), or go to the [journal homepage](#) for more

Download details:

IP Address: 129.252.86.83

The article was downloaded on 29/05/2010 at 16:45

Please note that [terms and conditions apply](#).

Ground states of model core-softened colloids

J Dobnikar¹, J Fornleitner² and G Kahl²

¹ Department of Theoretical Physics, Jožef Stefan Institute, Jamova 39, SI-1000 Ljubljana, Slovenia

² Center for Computational Materials Science and Institute for Theoretical Physics, Vienna University of Technology, Wiedner Hauptstrasse 8-10, A-1040 Vienna, Austria

E-mail: jure.dobnikar@ijs.si

Received 7 August 2008, in final form 8 September 2008

Published 12 November 2008

Online at stacks.iop.org/JPhysCM/20/494220

Abstract

We numerically study the condensed phases of repelling core-softened spheres confined to a planar cell at the crossover from two to three dimensions. In the related experiment presented in Osterman *et al* (2007 *Phys. Rev. Lett.* **99** 248301) the dipolar interaction between superparamagnetic spheres trapped in a thin cell was induced by a transverse magnetic field and tuned by adjusting the cell thickness. Depending on the cell thickness, the interaction can be purely repulsive (2D dipole–dipole), softened repulsive, or attractive at small distances. Clustering of colloids without any attractive force has been observed. Here we analyze the observed mesophases numerically by means of Monte Carlo simulations and by genetic algorithms based energy optimization. We observe the same phases seen in the experiment including expanded hexagonal, square, chain-like, stripe/labyrinthine, and honeycomb structures.

1. Introduction

The structures formed by idealized spherical colloids interacting via smooth, isotropic potentials have been well studied in the past. The spherical shape and the isotropy of the interparticle potential impose close-packed structures, i.e. the hexagonal and the face-centered cubic lattice [1, 2] in two and three dimensions, respectively. The surface treatment of particles [3], external fields [4] or a liquid-crystalline solvent [5] are a few examples where the interparticle interactions are anisotropic, resulting in richer phase diagrams. Alternatively, systems with isotropic pair interactions, but with a radial profile characterized by two length scales, also exhibit interesting phase behavior [6–12].

The simplest such system is composed of particles that interact via hard-core combined with penetrable-sphere repulsion (shoulder). If the shoulder/core diameter ratio exceeds about 2, this pair potential stabilizes a range of mesophases intervening between the fluid phase and the close-packed crystal. In two dimensions, the theoretical phase sequence includes loose- and close-packed hexagonal lattice; monomer, dimer, and trimer fluids; stripe and labyrinthine phases; honeycomb lattice, etc [6, 13, 14, 10]. Very similar behavior has been predicted numerically in the case of

paramagnetic particles confined to a plane and interacting with a dipolar repulsion induced by a transverse magnetic field and softened by a Lennard-Jones interaction [7]. For large shoulder/core diameter ratios, a universal set of mesophases is observed, including micellar, lamellar, and inverted micellar structure [15].

Recently an experiment with magnetic colloids has been performed [8] where the dipolar repulsion between the colloids was induced by an external magnetic field, whereas the spatial confinement of the system between two glass plates caused the softening of the radial profile of the interparticle interaction. The phase sequence observed in the experiment is very similar to the predictions in the above mentioned numerical simulations, showing that there is some kind of robustness—the details of the interparticle potential are not crucial as long as the potential features two length scales and has a concave shape at separations comparable to the nearest-neighbor distance.

In this paper we will present numerical results closely related to the experiment with magnetic colloids [8]. The paper is organized as follows: we start with the introduction of the model for confined magnetic colloids in the section *System* and continue with *Monte Carlo simulations*, *Energy minimization* and *Genetic algorithms* sections. Section *Conclusion* concludes the paper.

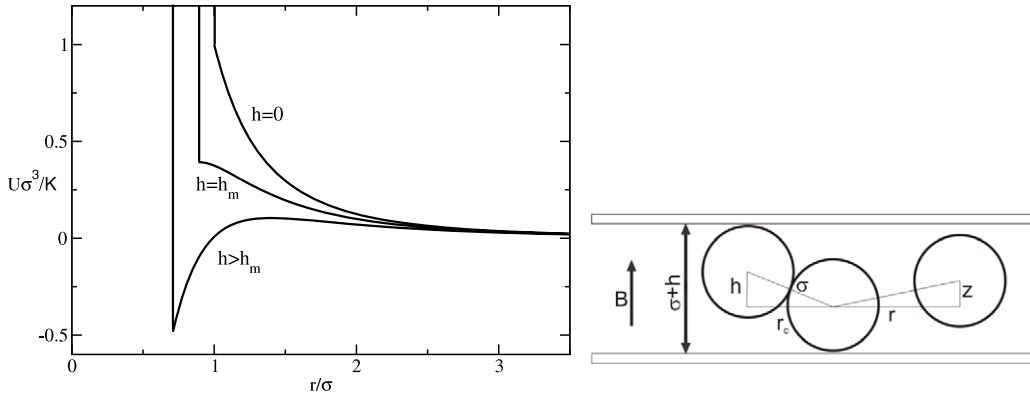


Figure 1. Left: the model interaction potential between two colloids confined to cells with three representative values of cell thickness and therefore three different values of the effective hard-core diameter r_c : at $h = 0$ and $r_c = \sigma$ (thin cell, circles) the potential has the form of pure 2D dipolar repulsion, at $h \approx h_m = \sigma/\sqrt{5}$ (squares) the repulsion is softened and the potential is flat at the contact (the effective hard-core diameter at this thickness is $r_c = 0.895\sigma$). At $h = 0.7\sigma > h_m$ and $r_c = 0.71\sigma$ (thick cell, triangles) the interaction is attractive at small separations. Right: a sketch of the system in cross-section.

2. System

The system consists of spherical micrometer-size magnetic colloids confined in the vertical direction as shown in the right-hand side of figure 1. The interaction is controlled by an external magnetic field inducing magnetic dipoles in the colloids. The interaction potential has the form

$$U(r, z) = K \frac{r^2 - 2z^2}{(r^2 + z^2)^{5/2}}, \quad (1)$$

where $K = \pi\sigma^6\chi^2B^2/(144\mu_0)$ is the interaction constant which depends on the magnetic induction B and the magnetic susceptibility χ of the particles; r and z are the in-plane and the vertical separations of the spheres, respectively (the vertical direction is defined by the direction of the external magnetic field), and σ is the diameter of the colloids (figure 1). The particles are allowed to buckle in the z direction, therefore their effective diameter r_c is smaller than σ :

$$r_c = \sqrt{\sigma^2 - h^2}. \quad (2)$$

In three dimensions the dipole–dipole interaction (1) is repulsive if the particles are at the same vertical position, but attractive if they are sufficiently displaced vertically. Two unconstrained colloids in three dimensions interacting via (1) would form a tower—one on top of another in the z direction. In two dimensions ($z = 0$), however, the interaction is purely repulsive with the typical $1/r^3$ radial dependence. If we control the vertical thickness of the system we have full control over interparticle interaction. It is convenient to denote the cell thickness by $\sigma + h$: thus h measures the deviation from a truly planar system. At finite h , the energetically favorable vertical arrangement of two particles is alternating: one colloid at the bottom plate and the other one at maximum distance at $z = h$. In the thin cells where $h \rightarrow 0$, U reduces to K/r^3 , whereas for $h > 0$ the relative vertical shift of the spheres reduces the repulsion at small distances. If $h > \sigma$ the situation is equivalent to that in three dimensions and the aforementioned tower configuration is stable.

The in-plane force between two particles is

$$F_r = -\partial U/\partial r = -3K \frac{r(4z^2 - r^2)}{(r^2 + z^2)^{7/2}}. \quad (3)$$

For two spheres in contact and keeping to the ‘top–bottom’ configuration in a cell of thickness $\sigma + h < 2\sigma$, the force is

$$F_r^c = -3K \frac{r_c(5h^2 - \sigma^2)}{\sigma^7}, \quad (4)$$

which becomes attractive for

$$h > h_m = \frac{\sigma}{\sqrt{5}} \approx 0.447\sigma. \quad (5)$$

In figure 1 the radial dependence of the interaction potential between two spheres for a range of h values is shown. The case with the cell thicknesses equal to $\sigma + h_m$ represents a purely repulsive system with interactions as soft as possible: the potential is flat (zero force) at the contact.

The experimentally observed mesophases in a system described by the above model have been published and discussed in detail in [8]. The most interesting phases experimentally observed at various 2D volume fractions $\eta = n\pi\sigma^2/4$ —where n is the 2D particle number density—include a fluid phase, an expanded hexagonal lattice, an expanded square lattice, a chain phase, stripe/labyrinthine structures, a honeycomb and a dense square lattice. They are remarkably close to those found in the numerical simulations reported in [7] although the pair interaction is not the same; a much more idealized hard-core/soft-shoulder interaction also gives a similar phase sequence [14, 6]. This suggests that the mechanisms at work as well as the structures they produce are rather robust.

3. Monte Carlo simulations

To understand the phase sequence in more detail, we performed 3D Monte Carlo simulations of up to $N = 1000$ spheres with the dipole–dipole pair repulsion in a cell of thickness $\sigma + h_m$.

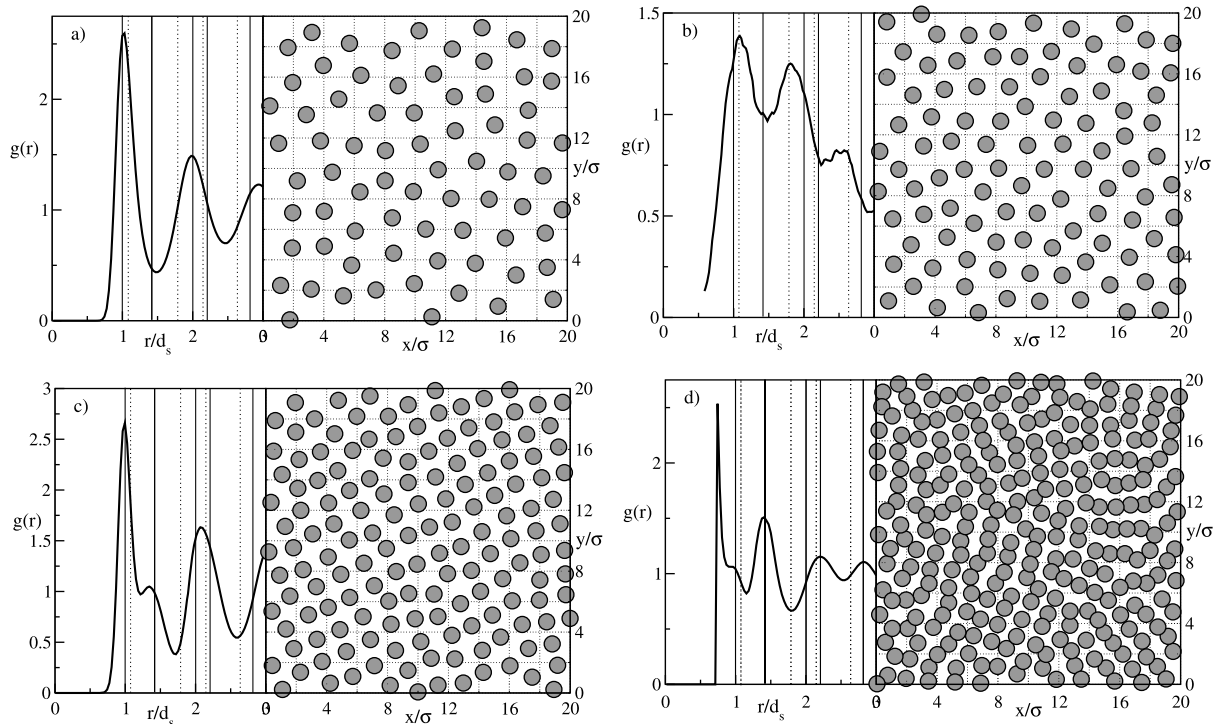


Figure 2. Radial distribution functions and typical snapshots from the Monte Carlo simulations at low temperature ($k = 400$). The values of the volume fraction are 0.15 (a), 0.20 (b), 0.30 (c) and 0.52 (d). The distance r on the $g(r)$ plots is in units of $d_s = \sqrt{\pi/\eta}$ which is the mean distance between the particles at a given volume fraction. The positions of the peaks of pure hexagonal and square lattices are marked by solid and dotted lines, respectively. In (a) the ground state is liquid, in (b) hexagonal, in (c) square, and in (d) chain-like. The simulated ground states agree very well with the experimentally measured mesophases [8].

We varied the volume fraction and we focused on the low temperature limit corresponding to large reduced interaction strengths $k = K/(k_B T \sigma^3)$; in the experiment, $k \approx 400$. We used periodic boundary conditions in several simulation box geometries; after reaching equilibrium (typically in a few million steps), 50×10^6 averaging steps were performed to evaluate the energy per particle and the radial distribution function. Some typical ground states and the corresponding radial distribution functions obtained through the simulations are shown in figure 2.

In the simulations the vertical positions of the spheres can be analyzed: at low volume fraction (less than about 0.05), they are uncorrelated and evenly distributed across the available range. However, for η larger than about 0.1 the distribution becomes bimodal with pronounced peaks corresponding to spheres touching the bottom or the top plate (figure 3). At high volume fractions where periodic structures are formed the system therefore resembles an off-lattice two-state spin ensemble with dominant nearest-neighbor antiferromagnetic interactions.

4. Energy minimization

The bimodal distribution of the vertical positions of colloids at high volume fractions allows us to treat the system as a binary system with two types of particles: those located at the bottom and the top wall, respectively. The up/down, up/up and down/down interactions are all known and we

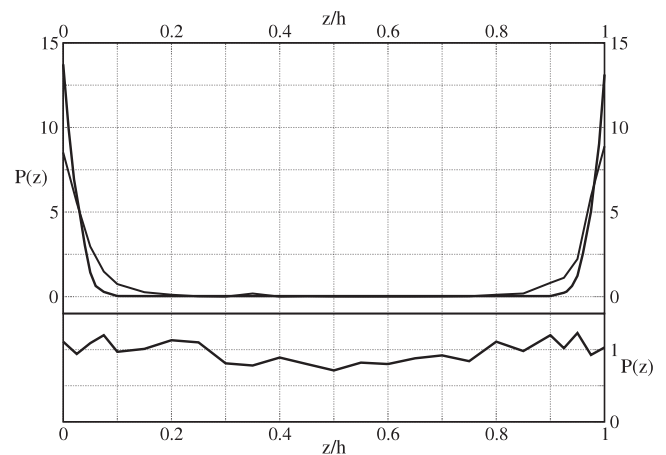


Figure 3. The distribution of the vertical positions of colloids in Monte Carlo simulations at $k = 400$. Top panel: $\eta = 0.45$ and 0.70 for the wider and the narrower distribution, respectively. Bottom panel: low volume fraction $\eta = 0.15$.

can compare the energies of various ground state candidate structures analytically. The ground states are dominated by the nearest-neighbor interactions—the nearest neighbors always tend to be of opposite type (up/down). The stripe, honeycomb, and square lattice with two, three, and four regularly arranged nearest neighbors, respectively, are compatible with alternating up–down positions of spheres, while the hexagonal lattice with six nearest neighbors is frustrated and no periodic ground state

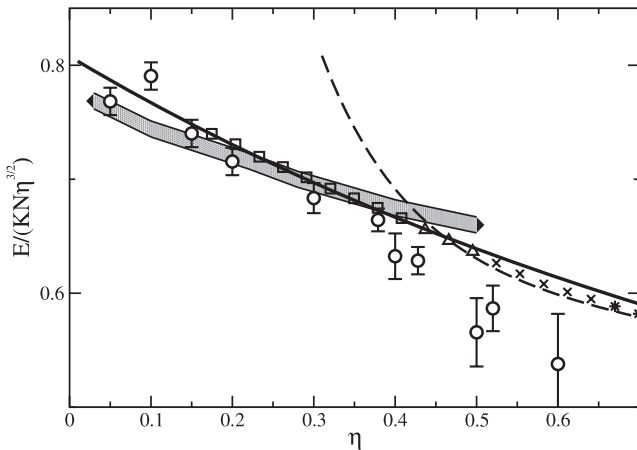


Figure 4. Energy per particle of the ground states of hexagonal (broad shaded line; the line thickness represents the numerical inaccuracy estimated by varying both the number of particles and the coupling constant), square (solid line), and stripe phase (dashed line) compared to the energies obtained by the full Monte Carlo simulation (open circles with error bars) and by the genetic algorithm optimization technique: the square lattice is denoted by squares; the dimer configuration by triangles, stripes by crosses and parameter sets for which the honeycomb lattice was obtained are marked by asterisks).

arrangement can be found. The energy of the hexagonal lattice was evaluated by fixing the particles' in-plane positions to a perfect hexagonal arrangement and annealing the vertical positions numerically. Systems of up to $N = 5000$ spheres have been analyzed corresponding to a cut-off of about 70 mean distances between the particles or between 200 and 300 particle diameters depending of course on the volume fraction. The ground states of the non-frustrated phases, such as the checkerboard structure of the square lattice, are ordered and unique, and their energies were calculated analytically using a lattice sum³. The results are shown in figure 4: at small η , the hexagonal phase has the lowest energy per particle among the three candidate phases, the square phase is stable at intermediate volume fractions, and at the largest volume fractions considered the stripes are energetically most favorable. In figure 4, we also plotted the energies of the equilibrium states obtained by the full Monte Carlo analysis that produced the snapshots shown in figure 2. Up to $\eta \approx 0.4$, the agreement of the energies calculated using lattice sums and simulations is quite good. In this regime, the simulations as well as the experiments usually produce coexistence of the hexagonal and the square lattice rather than a pure lattice (figure 2). This can be understood based on the lattice sum results which predict a very similar dependence of the energies of the two lattices on η , and thus the coexistence regime obtained by Maxwell construction should extend over a broad density range. At volume fractions beyond $\eta \approx 0.4$, the

³ We analyzed all stripe structures of width 1 by varying the intra-stripe separation, the stripe spacing, and the staggering of neighboring stripes. At any volume fraction, the minimal-energy configuration consists of close-packed stripes, and the neighboring stripes are out of register by one sphere diameter such that the stripe structure resembles a square lattice compressed along one lattice vector and stretched along the other one as much as possible.

difference between the energies of the model structures and those obtained by simulations slightly exceeds the error bar of the latter, suggesting that the stripe phase with perfectly parallel straight stripes is probably not the ground state and the many turns and junctions observed in experiment and simulation may be an equilibrium feature of the system.

5. Genetic algorithms

The symmetry of the phases observed in numerical simulations depends on the symmetry of the bounding box used. This problem can be circumvented by considering large systems and by comparing the stability of the phases in various bounding box shapes. Nevertheless, the issue remains, and the precise phase boundaries are very hard to determine. In addition, it is difficult to know if any other ground state exists at a particular box geometry not considered in our studies. We therefore also employ another, independent, method of investigation that does not share the difficulties of the Monte Carlo simulation: a search strategy based on the genetic algorithm approach to two-dimensional systems briefly discussed in [10]. For the present problem we had to make two assumptions (which will be verified *a posteriori*) and to extend the formalism as follows: the system is considered as a stacking sequence of n_1 parallel, two-dimensional ordered layers. It is *assumed* that the layers exhibit the same lattice and that the origin of layer i is displaced with respect to the origin of layer $(i - 1)$ by an interlayer vector c_i ; the origin of the bottom layer fixes the origin of the Cartesian coordinate system. Further, we postulate that the first layer is always located at the bottom of the cell (at $z = 0$) and that the n_1 th layer is located at the highest position ($z = h$). The z -components of the interlayer vectors, $c_{z,i}$, thus have to fulfil the condition

$$\sum_{i=1}^{n_1-1} c_{z,i} = h. \quad (6)$$

The two-dimensional lattice structure of the monolayers is described in the usual way (for details cf [10]), introducing two lattice vectors \mathbf{a} and \mathbf{b} and n_b position vectors for the particles in the unit cell. \mathbf{a} is assumed to be parallel to the x axis, thus \mathbf{b} is uniquely determined by the angle ϕ between the two vectors, and $\xi = |\mathbf{b}|/|\mathbf{a}|$; the first basis particle is assumed to be located at the origin of the unit cell. In total we have two parameters that fix the unit cell, ϕ and ξ , $2(n_b - 1)$ quantities describing the positions of the particles in the unit cell within one layer, and $3(n_1 - 1) - 1$ parameters for the components of the $(n_1 - 1)$ interlayer vectors. All of these parameters are optimized simultaneously in order to minimize the free energy of the layer system, which, at $T = 0$, reduces to the lattice sum of the crystal. The particle density and thus the packing fraction of the system is the only external parameter.

Both assumptions introduced above have been found to hold true. First, the fact that we encounter the same crystal structures in all layers could be verified by comparing the pair distribution functions obtained via simulations for all layers. These functions, originating from different layers, were found to match to a high precision. Second, previous investigations of the current system with the genetic algorithm, using a

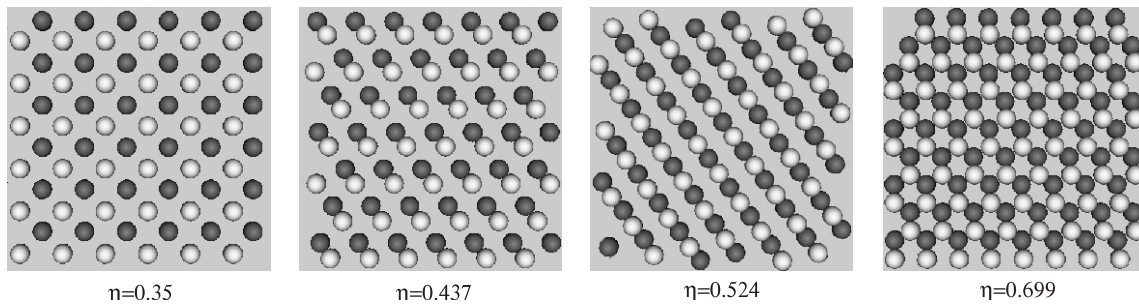


Figure 5. Sequence of typical structures found with the genetic algorithm technique as ordered minimum energy configurations of colloids in a cell of thickness $h = 0.445\sigma$: square lattice ($\eta = 0.35$), oblique lattice of dimers ($\eta = 0.437$), stripe lattice ($\eta = 0.524$), and honeycomb lattice ($\eta = 0.699$). The vertical position of the colloids is color-coded—black and white spheres are at the top and bottom plate, respectively.

parametrization where the vertical position of *every* particle in the unit cell could be optimized independently within the boundaries $z = 0$ and h , gave evidence that the particles are always either at the top and or at the bottom of the cell, thereby maximizing the distance between nearest neighbors. These two findings justified *a posteriori* our use of the above outlined parametrization of the system which is considerably less time-consuming and exhibits a better convergence.

We believe a combination of both methods—simulation and an optimization technique—to improve the reliability of our present and future surveys, e.g. by determining the optimal shape of the simulation box for the Monte Carlo simulation via a preceding genetic algorithm study of the system.

In this study, we have limited the maximum number of particles per two-dimensional unit cell to $n_b = 8$ and the maximum number of layers to $n_l = 4$. Due to the long-range nature of the interparticle potential, we have extended the lattice sums to distances as large as 200 times the particle diameter. The packing fractions for which we have determined minimum energy configurations range between $\eta = 0.175$ and 0.7, with a step-size of $\Delta\eta \approx 0.029$ and 0.006 in regions where structural change was encountered. In an effort to check the convergence and the reliability of our algorithm, we have performed 10 to 40 independent runs for every state point, depending on the numbers of parameters to optimize. For the current system of core-softened colloids in a cell of thickness $h + \sigma = 1.445\sigma$, we obtained a sequence of minimum energy configurations running from square lattices over a phase in which particles at opposite plates form pairs, to lane structures and arrive at honeycomb lattice for large values of η (see figure 5). The resulting energies of the structures are shown in figure 4. We find reasonable agreement with both the ground state energy calculations and the Monte Carlo numerical simulations. At the low volume fraction end of the presented GA results we cannot expect to observe the hexagonal structure found by the other two methods, since the hexagonal lattice is frustrated and no periodic ground state exists. The pair structure at $\eta = 0.437$ is also observed in the simulations as well as in the experiment, although not as clearly as in the GA search—we typically observed smaller domains of orientationally disordered pairs, probably due to the fact that our simulations and the experiment have not been performed at zero temperature.

6. Conclusion

We reported on experimental [8] and theoretical studies where a core-softened repulsive interaction was induced in micrometer-sized colloidal particles using the external magnetic field and fine-tuned by controlling the spatial constraints [8]. Depending on the density, the system forms several self-assembled mesophases—a square, hexagonal, and honeycomb lattice as well as a labyrinthine structure. The experiment [8] and our related numerical work validate many previously published predictions pertaining to similar pair interactions [14, 6, 7].

Acknowledgments

This work was supported by the Slovenian Research Agency (JD, grant P1-0055) and the Austrian Research Foundation (GK and JF, P17823-N08 and P19890-N16). We would like to thank Dušan Babič, Natan Osterman and Igor Poberaj (Ljubljana) for conducting the experiments [8] that motivated our work, Primož Zihelr (Ljubljana) for carefully reading the manuscript, Samir El Shawish (Ljubljana) for technical assistance and Mario Kahn (Vienna) for helpful discussions on using genetic algorithms for layered systems.

References

- [1] Kremer K, Robbins M O and Grest G S 1986 *Phys. Rev. Lett.* **57** 2694
- [2] Mau S C and Huse D A 1999 *Phys. Rev. E* **59** 4396
- [3] Nelson D R 2002 *Nano Lett.* **2** 1125
- [4] Yethiraj A and van Blaaderen A 2003 *Nature* **421** 513
- [5] Stark H 2001 *Phys. Rep.* **351** 387
- [6] Malescio G and Pellicane G 2003 *Nat. Mater.* **2** 97
- [7] Camp P J 2003 *Phys. Rev. E* **68** 061506
- [8] Osterman N, Babič D, Poberaj I, Dobnikar J and Zihelr P 2007 *Phys. Rev. Lett.* **99** 248301
- [9] Franzese G and Stanley H E 2008 *Water and Life: The Unique Properties of Water* ed R M Lynden-Bell, S Conway Morris, J D Barrow, J L Finney and C Harper (London: Taylor and Francis)
- [10] Fornleitner J and Kahl G 2008 *Europhys. Lett.* **82** 18001
- [11] Pauschenwein G J and Kahl G 2008 *Soft Matter* **4** 1396
- [12] Pauschenwein G J and Kahl G 2008 *J. Chem. Phys.* submitted (Pauschenwein G J and Kahl G 2008 arXiv:0808.0687v1 [cond-mat.soft])
- [13] Norioze Y and Kawakatsu T 2005 *Europhys. Lett.* **72** 583
- [14] Jagla E A 1999 *J. Chem. Phys.* **110** 451
- [15] Glaser M, Grason G M, Kamien R D, Košmrlj A, Santangelo C D and Zihelr P 2007 *Europhys. Lett.* **78** 46004 1998